05,10

Nutation resonance in different states of an antiferromagnet switched by an external magnetic field

© S.V. Titov[1], A.S. Fedorov[2,3], A.S. Titov[3], N.V. Chukashev[3]

[1] Kotel'nikov Institute of Radio Engineering and Electronics, Russian Academy of Sciences, Fryazino Branch, Fryazino, Moscow Region, Russia
[2] Kotelnikov Institute of Radio Engineering and Electronics, Russian Academy of Sciences, Moscow, Russia
[3] Moscow Institute of Physics and Technology, Institutsky lane 9, Dolgoprudny, Moscow region 141700, Russia

E-mail: pashkin1212@yandex.ru

Received October 27, 2024
Revised November 28, 2024
Accepted November 28, 2024

The results of a study of nutation resonances caused by the magnetization inertia of an antiferromagnet with two sublattices, possessing uniaxial magnetocrystalline anisotropy, are presented. Analytical expressions for the eigenfrequencies of the antiferromagnet are obtained by linearizing the system of coupled inertial Landau-Lifshitz-Gilbert equations describing the dynamics of the sublattice magnetizations. Various states of the antiferromagnet determined by the magnitude of the external magnetic field are considered for longitudinal (along the easy axis) and transverse directions of the field. The effect of dissipation in the system on the half-widths of the nutation resonance lines is demonstrated.

Keywords: antiferromagnet, ferromagnet, nutation resonance, antiferromagnetic resonance, Landau-Lifshitz-Gilbert equation, magnetization inertia, uniaxial magnetocrystalline anisotropy.

DOI: 10.61011/PSS.2025.01.60593.283

1. Introduction

The study of the magnetization dynamics of antiferromagnets (AFMs) is important because of the significant role it plays in various fields of science and technology, such as spintronics, magnonics, biomedical applications, etc. [1–5]. The concept of a magnetic structure of the antiferromagnetic type was proposed by Néel and Landau [6,7]. The basic theory, according to which antiferromagnets consist of sublattices with antiparallel orientation of magnetic moments, was developed by Néel [8–11]. The dynamics of the magnetization of each of the sublattices obeys the Landau-Lifshitz-Gilbert equation (LLG) [2,6].

The development of terahertz (THz) technologies [12], and the advancement of ultrafast memory based on spin systems [13,14] require studying the dynamics of magnetization over ultrashort time intervals. Thus, the possibility of switching the magnetization of an AFM by femtosecond laser pulses was discussed in Refs. [14,15]. Theoretical studies have shown that it is necessary to take into account the inertia of the magnetization when describing ultrafast relaxation processes and ultrahigh-frequency properties of magnetic materials [16,17]. The inertia of the magnetization changes the nature of the motion of the magnetization vector, namely, the nutation motion is superimposed on the regular precession around the effective field [18–22]. The nutation of the magnetization vector is caused by a continuous redistribution of a small fraction of the energy (since the inertia is quite small) from potential to kinetic and back during the motion. The nutational nature of the motion of the magnetization vector is reflected in the occurrence of a nutation resonance (NR) in the THz part of the spectra of the components of the susceptibility tensor of the magnetic material. In addition, if the time of external exposure is so short that the orientation of the magnetization virtually does not change during exposure, the magnetization, due to the presence of inertia, can acquire kinetic energy sufficient to overcome the potential barrier between metastable states after the end of exposure. This mechanism of magnetization switching becomes especially relevant on femtosecond time scales [16]. In this case, the choice of optimal switching parameters of the activating pulse directly depends on the dynamic characteristics of the magnetization.

The role of inertia of magnetization has been theoretically studied in ferromagnets (FMs) [22–25], AFMs [26,27], as well as in the formation of nutation waves [28–31]. Only recently the most convincing experimental data on the observation of NR at THz frequencies have been presented for ferromagnetic films NiFe, CoFeB [32,33] and for Co films [34]. The inertial dynamics of the magnetization of antiferromagnetic particles can differ in many ways from ferromagnetic particles due to properties inherent in antiferromagnetic materials. The AFM resonant frequencies shift into the high-frequency region of the spectrum due to the exchange interaction even in the non-inertial limit [6,26]. The frequencies of NR associated with the inertia of magnetization in AFMs can also shift to the high-frequency region of the spectrum [27].

AFMs with two sublattices are considered next. The inertial dynamics of the magnetizations $\mathbf{M}_i$ $(i = 1, 2)$ of the AFM sublattices coupled by exchange interaction can be described by a system of interrelated LLG equations supplemented by inertial terms [18–22] containing second-order time derivatives of the magnetizations, namely

$$\dot{\mathbf{M}}_i = \gamma_i \left[\mathbf{H}_i^{\text{eff}} \times M_i\right] + \frac{\alpha_i}{M_i^0}\left[\mathbf{M}_i \times \dot{\mathbf{M}}_i\right] + \frac{\tau_i}{M_i^0}\left[\mathbf{M}_i \times \ddot{\mathbf{M}}_i\right], \tag{1}$$

where $M_i^0 = |\mathbf{M}_i|$ is the length of the magnetization vector that does not change during the motion, $\mathbf{H}_i^{\text{eff}}$ is the effective magnetic field, γ_i is the gyromagnetic ratio, α_i is the dimensionless dissipation parameter, and τ_i is the inertial relaxation time of the ith sublattice ($\tau_i = \tau$ for identical sublattices). Theoretical models confirming the inertial behavior of magnetization described by the inertial term in Eq. (1) have been developed in addition to the phenomenological approach to accounting for the inertia of magnetization (see, for example, [18,22]). In particular, they include studies based on the calculation of the torque correlation [35], on the generalization of the Fermi surface model [36], on the application of the electronic structure analysis method [37], on the consideration of relativistic spin dynamics [38], and others. The value of the parameter τ associated with the inertial term plays an important role, since it is necessary to take into account the effects caused by the inertial term on sufficiently small time scales (smaller than τ) [32]. Recent theoretical studies show a significant variation in estimates of τ, ranging from tens of femtoseconds to tens of picoseconds [18,20,37–40]. A more precise value of this parameter is determined experimentally [32], for example, based on the magnetization nutation recorded in ferromagnetic thin films with an extremely high frequency $f_n = \omega_n/2\pi$, which is several orders of magnitude higher than the Larmor precession frequency, namely $f_n \sim 0.5\,\text{THz}$ ($\tau \sim (2\pi f_n)^{-1} \sim 0.3\,\text{ps}$) for NiFe, CoFeB films [32] and $f_n \sim 2.09$, 1.40, 1.31 THz ($\tau \sim 0.76$, 0.11, 0.12 ps) for Co films with three different types of crystal lattices [34]. The effective magnetic field $\mathbf{H}_i^{\text{eff}}$ of i-th sublattice in the Eq. (1) is defined in terms of the free energy density of the magnetic material $V(\mathbf{M}_1, \mathbf{M}_2)$ as

$$\mathbf{H}_i^{\text{eff}} = -\frac{1}{\mu_0}\frac{\partial V(\mathbf{M}_1, \mathbf{M}_2)}{\partial \mathbf{M}_i}, \tag{2}$$

where $\mu_0 = 4\pi \cdot 10^{-7}\,\text{J/(A}^2\text{m)}$ in the international SI system of units. The function $V(\mathbf{M}_1, \mathbf{M}_2)$ has several local minima [6], the positions of which depend on the strength of the external magnetic field. It is not only the positions of the minima that can change with a change in the strength of the external field, but also their number, which allows identifying several different states of the AFM [6].

Although the inertial equation of LLG has been successfully used to study NR in FM [18–25], a limited number of papers have been devoted to the study of the effect of inertia on the frequencies of antiferromagnetic resonance and NR in an AFM [26,27]. For instance, only one of the possible AFM states in a uniform external field is considered in [26], namely, a state corresponding to a weak external field applied along the easy axis of the sublattice in the approximation of two identical AFM sublattices. Changes of the AFM state due to changes in the magnitude of the external field („spin-flop“ and „spin-flip“ transitions) were not considered in Ref. [26]. Expressions for the eigenfrequencies of an AFM were obtained in Ref. [27] in the approximation of a negligible dissipation $\alpha_i \to 0$.

We analyze in this paper the effect of the inertial dissipative ($\alpha_i \neq 0$) dynamics of the magnetization of AFM sublattices, located in a uniform external field of arbitrary strength, on its spectral characteristics. In particular, we use the general method of theoretical mechanics to study small oscillations in the coordinates of complex systems characterizing the position of the system through the linearization of their related dynamic equations [6]. In our case, this approach allows one to obtain analytical expressions for the eigenfrequencies of the AFM, which, in turn, determine the frequencies of the antiferromagnetic (now inertia-corrected) and nutation resonances in all possible AFM states corresponding to different values of the external field [6]. The method was successfully applied earlier to estimate NR frequencies in single-domain ferromagnetic nanoparticles and in ferromagnetic films [23,41]. In this paper we consider an AFM with two sublattices of the ferromagnetic type having uniaxial magnetocrystalline anisotropy with parallel easy axes. This type of magnetocrystalline anisotropy is widely used in basic models for studying relaxation processes in magnets and materials [6,42]. We consider two main directions of the external field, namely along and across the special (easy) axis of the internal anisotropic potential of the sublattices, and analyze the dependence of the nutation frequencies on the strength of the external field. Moreover, we demonstrate how the inertial relaxation time affects the precession and nutation frequencies, increasing or decreasing them depending on the AFM state. The contribution of the dissipation parameter to the half-widths of the NR lines is also discussed.

2. Eigenfrequencies of small oscillations of the magnetization components of the AFM sublattices in the inertial regime

Solving coupled equations, Eq. (1), is an important point in the theory of magnetic oscillations in AFM. To find solutions of vector Eqs. (1) it is convenient to transform them into a system of scalar equations for spherical coordinates of the magnetizations of $\mathbf{M}_i$ of the sublattices, which have the form

$$\tau\ddot{\vartheta}_i - \dot{\varphi}_i \sin\vartheta_i - \tau\dot{\varphi}_i^2 \cos\vartheta_i \sin\vartheta_i + \partial_{\vartheta_i}\overline{V} + \alpha\dot{\vartheta}_i = 0, \tag{3}$$

$$\tau\ddot{\varphi}_i \sin\vartheta_i + \dot{\vartheta}_i + 2\tau\dot{\vartheta}_i\dot{\varphi}_i \cos\vartheta_i + \frac{1}{\sin\vartheta_i}\partial_{\varphi_i}\overline{V} + \alpha\dot{\varphi}_i \sin\vartheta_i = 0, \tag{4}$$

where ϑ_i and φ_i are the polar and azimuthal angles of the spherical coordinate system defining the orientations of the magnetizations $\mathbf{M}_i$, and $\overline{V} = \gamma V/(\mu_0 M_0)$ is the normalized free energy density function. We consider an AFM with identical sublattices in Eqs. (3) and (4), for simplicity, and neglect the difference of the length of the vectors $\mathbf{M}_i$, so that $|\mathbf{M}_i| = M_i^0 = M_0$, $\gamma = \gamma_i$, $\tau = \tau_i$, and $\alpha = \alpha_i$.

We find the eigenfrequencies of small orientation oscillations of the components of the vectors $\mathbf{M}_1$ and $\mathbf{M}_2$ by studying the case of their small deviations from stable orientations (minima of free energy density). In this case, the coordinates of these vectors make small oscillations near the angular coordinates $\vartheta_i^{\min}$ and $\varphi_i^{\min}$, corresponding to the minima of the function $V(\vartheta_1, \varphi_1, \vartheta_2, \varphi_2)$, namely $\vartheta_i(t) = \vartheta_i^{\min} + \Delta\vartheta_i(t)$ and $\varphi_i(t) = \varphi_i^{\min} + \Delta\varphi_i(t)$. Substituting these expressions into Eqs. ((3) and (4) and discarding the terms nonlinear in $\Delta\vartheta_i$ and $\Delta\varphi_i$, we obtain a system of eight linear differential equations for eight variables $\Delta\vartheta_i$, $\Delta\varphi_i$, ω_{ϑ_i} and ω_{φ_i} $(i = 1, 2)$, namely, $\Delta\dot{\vartheta}_i = \omega_{\vartheta_i}$, $\Delta\dot{\varphi}_i = \omega_{\varphi_i}$ and

$$\dot{\omega}_{\vartheta_i} = \frac{1}{\tau}\,\omega_{\varphi_i}\sin\vartheta_i - \frac{\alpha}{\tau}\,\omega_{\vartheta_i} - \frac{1}{\tau}\sum_{j=1,\,2}\left(\overline{V}_{\vartheta_i\vartheta_j}\Delta\vartheta_j + \overline{V}_{\vartheta_i\varphi_j}\Delta\varphi_j\right), \tag{5}$$

$$\dot{\omega}_{\varphi_i} = -\frac{1}{\tau\sin\vartheta_i}\,\omega_{\vartheta_i} - \frac{\alpha}{\tau}\,\omega_{\varphi_i} - \frac{1}{\tau\sin^2\vartheta_i} \times \sum_{j=1,\,2}\left(\overline{V}_{\varphi_i\vartheta_j}\Delta\vartheta_j + \overline{V}_{\varphi_i\varphi_j}\Delta\varphi_j\right). \tag{6}$$

All functions and derivatives $\overline{V}_{x_i x_j}$ are calculated for $\vartheta_i = \vartheta_i^{\min}$ and $\varphi_i = \varphi_i^{\min}$ in Eqs. (5) and (6). This condition guarantees that for the function $V(\vartheta_1, \varphi_1, \vartheta_2, \varphi_2)$ all its derivatives with respect to ϑ_i and φ_i at the point $\boldsymbol{\theta}_{\min} = \{\vartheta_1^{\min}, \varphi_1^{\min}, \vartheta_2^{\min}, \varphi_2^{\min}\}$ of four-dimensional space are zero, namely $\overline{V}_{\vartheta_i}\big|_{\boldsymbol{\theta}_{\min}} = 0$ and $\overline{V}_{\varphi_i}\big|_{\boldsymbol{\theta}_{\min}} = 0$. The following linear approximations are used as a result

$$\frac{\partial\overline{V}}{\partial\vartheta_i} \approx \sum_{j=1}^{2}\left(\frac{\partial^2\overline{V}}{\partial\vartheta_i\partial\vartheta_j}\bigg|_{\boldsymbol{\theta}_{\min}}\Delta\vartheta_j + \frac{\partial^2\overline{V}}{\partial\vartheta_i\partial\varphi_j}\bigg|_{\boldsymbol{\theta}_{\min}}\Delta\varphi_j\right), \tag{7}$$

$$\frac{\partial\overline{V}}{\partial\varphi_i} \approx \sum_{j=1}^{2}\left(\frac{\partial^2\overline{V}}{\partial\varphi_i\partial\vartheta_j}\bigg|_{\boldsymbol{\theta}_{\min}}\Delta\vartheta_j + \frac{\partial^2\overline{V}}{\partial\varphi_i\partial\varphi_j}\bigg|_{\boldsymbol{\theta}_{\min}}\Delta\varphi_j\right). \tag{8}$$

The system of linear differential equations can be reduced to a matrix equation

$$\mathbf{C}(t) + \mathbf{A}\mathbf{C}(t) = 0, \tag{9}$$

where the vector $\mathbf{C}(t)$ consists of eight variables, namely

$$\mathbf{C}(t) = \left(\Delta\vartheta_1(t), \Delta\varphi_1(t), \Delta\vartheta_2(t), \Delta\varphi_2(t), \omega_{\vartheta_1}(t), \omega_{\varphi_1}(t), \omega_{\vartheta_2}(t), \omega_{\varphi_2}(t)\right)^T. \tag{10}$$

Here, the symbol „T“ means transposing a row into a column. The system matrix $\mathbf{A}$ includes four submatrices

$$\mathbf{A} = \begin{pmatrix}\mathbf{Z} & -\mathbf{I}\\ \mathbf{V} & \mathbf{D}\end{pmatrix}, \tag{11}$$

where $\mathbf{Z}$ and $\mathbf{I}$ are the zero and unit submatrices, respectively. The submatrix $\mathbf{V}$ is determined by the second derivatives of the function $V(\vartheta_1, \varphi_1, \vartheta_2, \varphi_2)$

$$\mathbf{V} = \frac{1}{\tau}\begin{pmatrix} \overline{V}_{\vartheta_1\vartheta_1} & \overline{V}_{\vartheta_1\varphi_1} & \overline{V}_{\vartheta_1\vartheta_2} & \overline{V}_{\vartheta_1\varphi_2} \\ \dfrac{\overline{V}_{\varphi_1\vartheta_1}}{\sin^2\vartheta_1} & \dfrac{\overline{V}_{\varphi_1\varphi_1}}{\sin^2\vartheta_1} & \dfrac{\overline{V}_{\varphi_1\vartheta_2}}{\sin^2\vartheta_1} & \dfrac{\overline{V}_{\varphi_1\varphi_2}}{\sin^2\vartheta_1} \\ \overline{V}_{\vartheta_2\vartheta_1} & \overline{V}_{\vartheta_2\varphi_1} & \overline{V}_{\vartheta_2\vartheta_2} & \overline{V}_{\vartheta_2\varphi_2} \\ \dfrac{\overline{V}_{\varphi_2\vartheta_1}}{\sin^2\vartheta_2} & \dfrac{\overline{V}_{\varphi_2\varphi_1}}{\sin^2\vartheta_2} & \dfrac{\overline{V}_{\varphi_2\vartheta_2}}{\sin^2\vartheta_2} & \dfrac{\overline{V}_{\varphi_2\varphi_2}}{\sin^2\vartheta_2} \end{pmatrix}, \tag{12}$$

whereas the matrix $\mathbf{D}$ is given as

$$\mathbf{D} = \frac{1}{\tau}\begin{pmatrix} \alpha & -\sin\vartheta_1 & 0 & 0 \\ \sin^{-1}\vartheta_1 & \alpha & 0 & 0 \\ 0 & 0 & \alpha & -\sin\vartheta_2 \\ 0 & 0 & \sin^{-1}\vartheta_2 & \alpha \end{pmatrix}. \tag{13}$$

Equation (9) has the general solution [43]

$$\mathbf{C}(t) = \exp[-\mathbf{A}t]\mathbf{C}(0) = \mathbf{U}e^{-\lambda t}\mathbf{U}^{-1}\mathbf{C}(0), \tag{14}$$

where λ is a diagonal matrix composed of the eigenvalues $\{\lambda_k\}$ of the system matrix $\mathbf{A}$, and $\mathbf{U}$ is a right-sided matrix composed of the eigenvectors of the matrix $\mathbf{A}$. The eigenvalues of the system $\lambda_k = -i\omega_k = -i(\omega_k' + i\omega_k'')$, which determine the oscillation frequencies ω_k' and their attenuation rate ω_k'', are found from the solution of the characteristic equation

$$\det(\mathbf{A} - \lambda\mathbf{I}) = 0. \tag{15}$$

If the exchange coupling between the sublattices is negligible, the variables in the free energy density are separated by $V(\vartheta_1, \varphi_1, \vartheta_2, \varphi_2) = V(\vartheta_1, \varphi_1) + V(\vartheta_2, \varphi_2)$, and the two sublattices behave like two independent FMs with similar equations for eigenvalues ($\vartheta_i = \vartheta$ and $\varphi_i = \varphi$), namely,

$$\lambda^2\left((\tau\lambda - \alpha)^2 + 1\right) + \frac{\gamma\lambda(\tau\lambda - \alpha)}{\mu_0 M_0}\left(V_{\vartheta\vartheta} + \frac{V_{\varphi\varphi}}{\sin^2\vartheta}\right) + \frac{\gamma^2(V_{\vartheta\vartheta}V_{\varphi\varphi} - V_{\vartheta\varphi}^2)}{(\mu_0 M_0\sin\vartheta)^2} = 0 \tag{16}$$

The solution of Eq. (16) is given in Ref. [23] for $\alpha = 0$ and in Ref. [41] for $\alpha \neq 0$. The solution of Eq. (16) for $\alpha = 0$ gives the well-known Sula-Smith formula for ferromagnetic resonance frequencies in the non-inertial limit $\tau = 0$ [6].

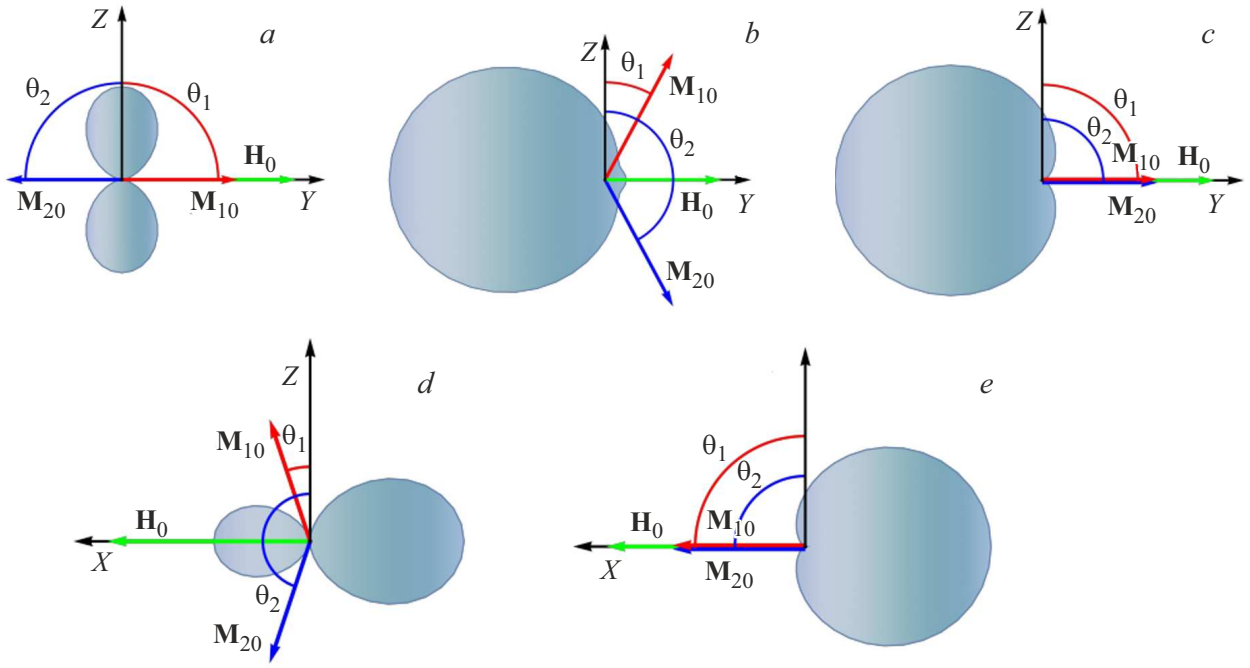

Figure 1. Geometry of the problem: $a-c$ — the easy axis is directed along the Y-axis, $\mathbf{n} = \mathbf{e}_Y$, the external field is directed along the easy axis $\mathbf{H}_0 = H_0\mathbf{e}_Y$; d, e — the easy axis is directed along the Z-axis, $\mathbf{n} = \mathbf{e}_Z$, the external magnetic field $\mathbf{H}_0$ is applied perpendicular to the easy axis $\mathbf{H}_0 = H_0\mathbf{e}_X$.

3. Solution of the characteristic equation for the longitudinal and transverse directions of the external field

Next, we consider an AFM with two sublattices having one axis of cyclic symmetry of the magnetocrystalline anisotropic potential (uniaxial magnetic anisotropy). In the general case, the energy density $V(\mathbf{M}_1, \mathbf{M}_2)$ of the AFM in a uniform external magnetic field $\mathbf{H}_0$ consists of the densities of the exchange energy, the energy of interaction with the internal field due to magnetic anisotropy, and the energy of the Zeeman interaction with the external field. The energies of interaction with the internal and external fields are composed of the corresponding energies of each sublattice of the AFM. If we take $\mathbf{n}$ as a unit vector along the easy axis of the AFM, then the free energy density $V(\mathbf{M}_1, \mathbf{M}_2)$ is equal to [6,26]

$$V(\mathbf{M}_1, \mathbf{M}_2) = \frac{\Lambda}{M_0^2}\mathbf{M}_1 \cdot \mathbf{M}_2 - \sum_{i=1,2}\left(K\frac{(\mathbf{M}_i \cdot \mathbf{n})^2}{M_0^2} + \mu_0\mathbf{H}_0 \cdot \mathbf{M}_i\right). \quad (17)$$

where Λ is the parameter of the exchange interaction between the sublattices, and $K = K_i$ is the constant of uniaxial anisotropy of the sublattices.

We are interested in two cases when the external magnetic field is directed along the easy axis ($\mathbf{H}_0 = H_0\mathbf{e}_Y$ and $\mathbf{n} = \mathbf{e}_Y$) and perpendicular to it ($\mathbf{H}_0 = H_0\mathbf{e}_X$ and $\mathbf{n} = \mathbf{e}_Z$) (see Figure 1). Here $\mathbf{e}_X$, $\mathbf{e}_Y$ and $\mathbf{e}_Z$ are unit vectors along the axes X, Y and Z, respectively. The positions of the minima of the function $V(\mathbf{M}_1, \mathbf{M}_2)$ (or the orientations of the stable positions of the magnetizations $\mathbf{M}_{10}$ and $\mathbf{M}_{20}$ of the sublattices corresponding to the coordinates of the minima $\vartheta_i^{\min}$ and $\varphi_i^{\min}$) vary depending on the magnitude of the field $\mathbf{H}_0$. Moreover, three different states are possible in the case when the field $\mathbf{H}_0$ is directed along the easy axis (Figure 1, $a-c$), and two different states are possible in the case when the field $\mathbf{H}_0$ is perpendicular to the easy axis (Figure 1, d and 1, e) [6].

The normalized free energy density $\overline{V}$ in a spherical coordinate system has the form

$$\overline{V}_{\parallel} = \omega_\Lambda(\sin\vartheta_1 \sin\vartheta_2 \cos(\varphi_1 - \varphi_2) + \cos\vartheta_1 \cos\vartheta_2) - \sum_{i=1,2}\left(\frac{\omega_K}{2}\sin^2\vartheta_i \sin^2\varphi_i + \omega_0 \sin\vartheta_i \sin\varphi_i\right) \quad (18)$$

for $\mathbf{H}_0 \parallel \mathbf{n}$ and

$$\overline{V}_{\perp} = \omega_\Lambda(\sin\vartheta_1 \sin\vartheta_2 \cos(\varphi_1 - \varphi_2) + \cos\vartheta_1 \cos\vartheta_2) - \sum_{i=1,2}\left(\frac{\omega_K}{2}\cos^2\vartheta_i + \omega_0 \sin\vartheta_i \cos\varphi_i\right) \quad (19)$$

for $\mathbf{H}_0 \perp \mathbf{n}$, where $\omega_\Lambda = \gamma H_\Lambda$, $H_\Lambda = \Lambda/(\mu_0 M_0)$ is a field due to the exchange interaction of sublattices, $\omega_K = \gamma H_K$, $H_K = 2K/(\mu_0 M_0)$ is a field due to magnetic anisotropy, and $\omega_0 = \gamma H_0$ is the Larmor precession frequency in an external magnetic field.

It follows from the symmetry of the problem that the stable directions of the magnetization $\mathbf{M}_{10}$ and $\mathbf{M}_{20}$, the

Table 1. States of the AFM and the positions of the minima in them

Field direction	Range of field values (Figure 1)	Positions of minima
$\mathbf{H}_0 \parallel \mathbf{n}$	$(a)\ 0 < H_0 < \sqrt{H_K H_+^C}$	$\vartheta_1^{\min_a} = \vartheta_2^{\min_a} = \pi/2,\ \varphi_1^{\min_a} = \pi/2,\ \varphi_2^{\min_a} = 3\pi/2$
	$(b)\ \sqrt{H_K H_-^C} < H_0 < H_-^C$	$\vartheta_1^{\min_b} = \arcsin[\omega_0/\omega_-^C],\ \vartheta_2^{\min_b} = \pi - \vartheta_1^{\min_b},$ $\varphi_1^{\min_b} = \varphi_2^{\min_b} = \pi/2$
	(c) $H_0 > H_-^C$	$\vartheta_1^{\min_c} = \vartheta_2^{\min_c} = \pi/2,\ \varphi_1^{\min_c} = \varphi_2^{\min_c} = \pi/2,$
$\mathbf{H}_0 \perp \mathbf{n}$	$(d)\ 0 < H_0 < H_+^C$	$\vartheta_1^{\min_d} = \arcsin[\omega_0/\omega_+^C],\ \vartheta_2^{\min_d} = \pi - \vartheta_1^{\min_d},$ $\varphi_1^{\min_d} = \varphi_2^{\min_d} = 0$
	(e) $H_+^C < H_0$	$\vartheta_1^{\min_e} = \vartheta_2^{\min_e} = \pi/2,\ \varphi_1^{\min_e} = \varphi_2^{\min_e} = 0,$

Table 2. Equations for eigenfrequencies in various states of the AFM

Figure 1.	Equation
(a)	$\big(\omega(\tau\omega - i\alpha) - \omega_+^C\big)\big(\omega(\tau\omega - i\alpha) - \omega_K\big) - (\omega_0 \pm \omega)^2 = 0$
(b)	$(\omega\tau - i\alpha)\big[\omega_0^2 - (\omega_-^C)^2\big] + \big[(\omega\tau - i\alpha)^2 - 1\big]\omega\omega_-^C = 0$ $(\omega_-^C)^2\big(\omega^2(\omega\tau - i\alpha)^2 - \omega^2 - (\omega\tau - i\alpha)\omega\omega_-^C - 2\omega_K\omega_\Lambda\big) - \omega_+^C\omega_0^2\big(\omega(\omega\tau - i\alpha) - 2\omega_\Lambda\big) = 0$
(c)	$\big(\omega(\tau\omega - i\alpha) - \omega_0 - \omega_K \pm \omega\big)\big(\omega(\tau\omega - i\alpha) - \omega_0 + \omega_-^C \pm \omega\big) = 0$
(d)	$\omega^2\big[(\omega\tau - i\alpha)^2 - 1\big](\omega_+^C)^2 + \omega_+^C\big(\omega_0^2\omega_-^C + (\omega_+^C)^2\omega_K\big) - \omega(\omega\tau - i\alpha)\big[\omega_0^2\omega_-^C + 2(\omega_+^C)^2(\omega_K + \omega_\Lambda)\big] = 0$ $\omega^2\big((\omega\tau - i\alpha)^2 - 1\big)\omega_+^C + \big((\omega_+^C)^2 - \omega_0^2\big)\omega_K + \omega(\omega\tau - i\alpha)\big(\omega_0^2 - 2\omega_+^C(\omega_K + \omega_\Lambda)\big) = 0$
(e)	$(\omega(\omega\tau - i\alpha) - \omega_0)^2 + (\omega(\omega\tau - i\alpha) - \omega_0)\omega_K - \omega^2 = 0$ $(\omega(\tau\omega - i\alpha) - \omega_0 + \omega_+^C)(\omega(\tau\omega - i\alpha) - \omega_0 + 2\omega_\Lambda) - \omega^2 = 0$

field $\mathbf{H}_0$ and the easy axis of magnetic anisotropy lie in the same plane [6]. The potentials $\overline{V}_{\parallel,\perp}(\vartheta_1, \varphi_1, \vartheta_2, \varphi_2)$, given by Eqs. (18) and (19), projected onto these planes, represent the closed lines shown in Figure 1 for all considered cases. These contours in polar coordinates $\{r, \theta\}$ are defined as

$$r_j(\theta) = \overline{V}_{\parallel,\perp}(\theta, \varphi_1^{\min_j}, \pi - \theta, \varphi_2^{\min_j}) - \overline{V}_{\parallel,\perp}(\boldsymbol{\theta}_{\min_j}), \quad (20)$$

where j=a, b, c, d, e, and $\boldsymbol{\theta}_{\min_j}$=$(\vartheta_1^{\min_j}, \varphi_1^{\min_j}, \vartheta_2^{\min_j}, \varphi_2^{\min_j})$ is the minimum point for the state j. A more general procedure for finding the minima and transitions between states with a change of the external field $\mathbf{H}_0$ is described, for example, in Ref. [6], where the non-inertial dynamics of magnetization is considered.

The positions of the minima corresponding to different directions and ranges of the external field strength $\mathbf{H}_0$ are listed in Table 1. For instance, the stable states of the magnetizations $\mathbf{M}_{10}$ and $\mathbf{M}_{20}$ have an antiparallel orientation in the case of a longitudinally directed relatively weak external field $(0 < H_0 < \sqrt{H_K H_+^C}$, where $H_\pm^C = \omega_\pm^C/\gamma = 2H_\Lambda \pm H_K)$ (not to be confused with the orientations of the magnetizations themselves $\mathbf{M}_1$ and $\mathbf{M}_2$) (Figure 1, a). A transition to a non-collinear state takes place as the field increases (Figure 1, b), which is known as „spin-flop“ transition [2,6].

Both states (a) and (b) are possible in the range of fields $\sqrt{H_K H_-^C} < H_0 < \sqrt{H_K H_+^C}$. This interval is quite narrow, since $H_K \ll H_\Lambda$ for most AFMs. For this reason it is possible ignore the difference between H_+^C and H_-^C and use the approximation $H_+^C \sim H_-^C \sim 2H_\Lambda$. With a further increase of the external field, the angle between the directions $\mathbf{M}_{10}$ and $\mathbf{M}_{20}$ decreases, and a transition takes place to the third state with parallel directions of $\mathbf{M}_{10}$ and $\mathbf{M}_{20}$ at $H_0 > H_-^C$ (Figure 1, c). This transition is known as „spin-flip“ [2,6]. MnF_2, $FeCl_2$, $GdAlO_3$, $K_2[FeCl_5(H_2O)]$, FeF_2 are examples of AFM in which „spin-flop“ and/or „spin-flip“ transitions were observed [2,6]. The field required for the „spin-flop“ transition to occur $(H_0 \sim \sqrt{2H_K H_\Lambda})$ varies from ~ 1 T ($GdAlO_3$) to ~ 42 T (FeF_2) [2,6]. The angle between $\mathbf{M}_{10}$ and $\mathbf{M}_{20}$ gradually decreases with the increase of H_0 in the case of the transverse direction of the uniform external field (Figure 1, d). A transition to a state with co-directional $\mathbf{M}_{10}$ and $\mathbf{M}_{20}$ takes place at $H_0 > H_+^C$ (Figure 1, e).

The AFM eigenfrequencies are found from the solution of the quartic equation in the presence of dissipation and an inertial term. These equations corresponding to the different states of the AFM are given in Table 2. The solutions of the equations are complex. They can be found analytically using, for example, the Ferrari method [44]. These solutions (precession frequencies $\omega_{1,2}^p$ and nutation frequencies $\omega_{1,2}^n$)

Table 3. Eigenfrequencies for different AFM states

Figure 1.	Frequencies
(a)	$\omega_{\pm}^{p} \approx \sqrt{\omega_K\omega_+^C} \pm \omega_0 - (\omega_K+\omega_\Lambda)\left(\sqrt{\omega_K\omega_+^C} \pm \omega_0\right)\left[\tau\left(\sqrt{\omega_K\omega_+^C} \pm \omega_0\right) - i\alpha\right]/\sqrt{\omega_K\omega_+^C}$ $\omega_{\pm}^{n} \approx \tau^{-1}(1-i\alpha) + \omega_K + \omega_\Lambda \pm \omega_0$
(b)	$\omega_1^{p,n} = \frac{1}{\sqrt{2\tau}}\sqrt{1+\tau\omega_-^C + \frac{\tau\omega_0^2\omega_+^C}{(\omega_-^C)^2} \mp D_1^{1/2}} + \frac{i\alpha}{2\tau}\left(1 \mp D_1^{-1/2}\right)$, $\omega_2^{p,n} = \frac{\delta_{1\mp1}}{\tau}D_2^{1/2} + \frac{i\alpha}{2\tau}(2-\delta_{1\mp1})\left(1 \mp D_2^{-1}\right)$, $D_1 = \left(1+\tau\omega_-^C + \frac{\tau\omega_0^2\omega_+^C}{(\omega_-^C)^2}\right)^2 + 8\tau^2\omega_\Lambda\left(\omega_K - \frac{\omega_0^2\omega_+^C}{(\omega_-^C)^2}\right)$, $D_2 = 1+\tau\omega_-^C - \frac{\tau\omega_0^2}{\omega_-^C}$
(c)	$\omega_1^{p,n} = \frac{\mp1+i\alpha+\sqrt{(1\mp i\alpha)^2+4\tau(\omega_0+\omega_K)}}{2\tau}$, $\omega_2^{p,n} = \frac{\mp1+i\alpha+\sqrt{(1\mp i\alpha)^2+4\tau(\omega_0-\omega_-^C)}}{2\tau}$,
(d)	$\omega_1^{p,n} = \frac{1}{\sqrt{2\tau}}\left(1+2\tau\left(\omega_+^C - \omega_\Lambda + \frac{\omega_0^2\omega_-^C}{2(\omega_+^C)^2}\right) \mp D_1^{1/2}\right)^{1/2} + \frac{i\alpha}{2\tau}\left(1 \mp D_1^{-1/2}\right) + O(\alpha^2)$ $\omega_2^{p,n} = \frac{1}{\sqrt{2\tau}}\left(1+2\tau\left(\omega_K + \omega_\Lambda - \frac{\omega_0^2}{2\omega_+^C}\right) \mp D_2^{1/2}\right)^{1/2} + \frac{i\alpha}{2\tau}\left(1 \mp D_2^{-1/2}\right) + O(\alpha^2)$ $D_1 = 4\tau\omega_+^C + \left(1+2\tau\left(\frac{\omega_0^2\omega_-^C}{2(\omega_+^C)^2} - \omega_\Lambda\right)\right)^2$, $D_2 = 4\tau\omega_K + \left(1+2\tau\left(\omega_\Lambda - \frac{\omega_0^2}{2\omega_+^C}\right)\right)^2$
(e)	$\omega_1^{p,n} = \frac{1}{\sqrt{2\tau}}(1+\tau(2\omega_0-\omega_K) \mp D_1^{1/2})^{1/2} + \frac{i\alpha}{2\tau}(1 \mp D_1^{-1/2}) + O(\alpha^2)$ $\omega_2^{p,n} = \frac{1}{\sqrt{2\tau}}(1+\tau(2\omega_0-\omega_K-4\omega_\Lambda) \mp D_2^{1/2})^{1/2} + \frac{i\alpha}{2\tau}(1 \mp D_2^{-1/2}) + O(\alpha^2)$ $D_1 = 4\tau\omega_0 + (1-\tau\omega_K)^2$, $D_2 = 4\tau\omega_0 + (1-\tau\omega_K)^2 - 8\tau\omega_\Lambda$

are provided in Table 3 in the form of a parameter expansion α with only the linear term for α for simplicity. The exceptions are cases (a) and (c). The complex solutions are simplified for the case (a) by the decomposition into two smallness parameters τ and α, whereas the general solutions have a simple form for the case (c). Since both experimental and theoretical estimates of the parameter α give values of the order of $0.001-0.1$ [42], it is sufficient to use the expressions from Table 3 for many computational purposes. It should be noted that the solutions presented for $\alpha = 0$ are consistent with the results obtained in Ref. [27], where the dissipation in the system was not considered, which made it possible to find the eigenfrequencies of the AFM from the solution of the second-order equation. Setting the inertial relaxation time τ to zero one obtains the well-known expressions for the frequencies of antiferromagnetic resonance [6].

4. Components of the susceptibility tensor

Let us consider the dynamics of the magnetization of the AFM sublattices under the impact of a weak alternating field $\mathbf{H}_\sim(t) = \mathbf{H}_\sim \exp[i\omega t]$, where the field amplitude is given as $\mathbf{H}_\sim = H_\sim(\sin\vartheta_\sim\cos\varphi_\sim, \sin\vartheta_\sim\sin\varphi_\sim, \cos\vartheta_\sim)$. In this case, the Zeeman energy in an alternating field will be added to the free energy density $V(\mathbf{M}_1, \mathbf{M}_2)$

$$\tilde{V}(\mathbf{M}_1,\mathbf{M}_2) = -\mu_0\mathbf{H}_\sim\cdot(\mathbf{M}_1+\mathbf{M}_2) = -\mu_0 M_0 H_\sim \exp[i\omega t] \times\sum_{i=1,2}(\cos\vartheta_\sim\cos\vartheta_i + \sin\vartheta_\sim\sin\vartheta_i\cos(\varphi_\sim-\varphi_i)). \tag{21}$$

The solution of Eqs. (3) and (4) is sought in the form $\vartheta_i(t) = \vartheta_i^{\min} + \Delta\vartheta_i\exp[i\omega t]$ and $\varphi_i(t) = \varphi_i^{\min} + \Delta\varphi_i\exp[i\omega t]$. After substituting these expressions into Eqs. (3) and (4) and their linearization, taking into accoun Eq. (21), we obtain a system of algebraic equations that can be represented in matrix form

$$(\omega^2\mathbf{I} - i\omega\mathbf{D} - \mathbf{V})\mathbf{X} = \mathbf{F}, \tag{22}$$

where

$$\mathbf{X} = \begin{pmatrix}\Delta\vartheta_1\\ \Delta\varphi_1\\ \Delta\vartheta_2\\ \Delta\varphi_2\end{pmatrix}, \quad \mathbf{F} = \frac{1}{\tau}\begin{pmatrix}\tilde{\overline{V}}_{\vartheta_1}\\ \sin^{-2}\vartheta_1\tilde{\overline{V}}_{\varphi_1}\\ \tilde{\overline{V}}_{\vartheta_2}\\ \sin^{-2}\vartheta_2\tilde{\overline{V}}_{\varphi_2}\end{pmatrix}. \tag{23}$$

Here we take into account that in the general case $\tilde{\overline{V}}_{\vartheta_i}\big|_{\boldsymbol{\theta}_{\min}} \neq 0$ and $\tilde{\overline{V}}_{\varphi_i}\Big|_{\boldsymbol{\theta}_{\min}} \neq 0$. It should be noted that the condition for having a nontrivial solution to a homogeneous system, namely $\det[\omega^2\mathbf{I} - i\omega\mathbf{D} - \mathbf{V}] = 0$, leads to the same solutions as Eq. (15), while the solutions of both equations

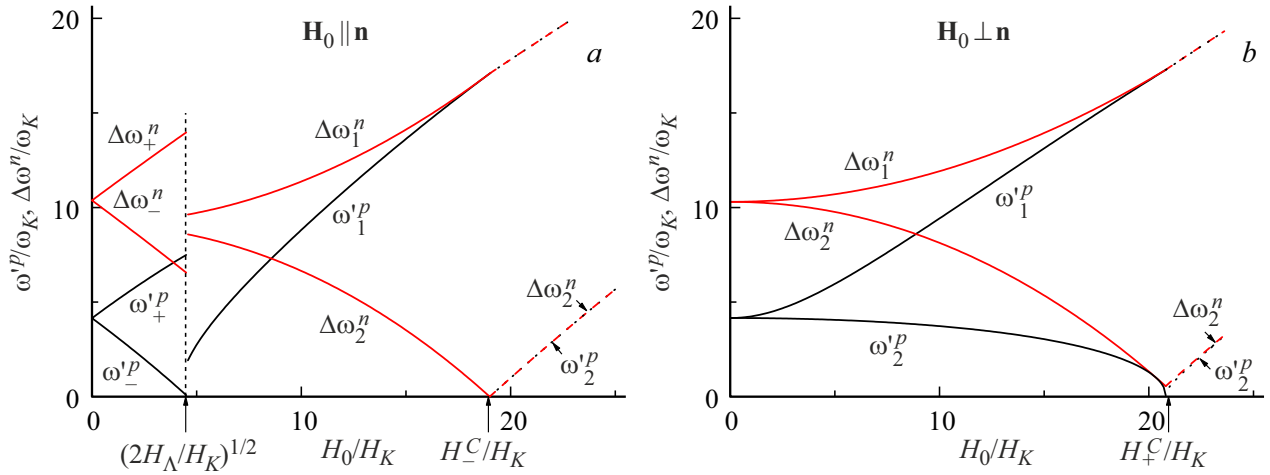

Figure 2. Precession frequency $\omega_i'^p = \mathrm{Re}[\omega_i^p]$ of the total magnetization of the AFM sublattices and the deviation of the magnetization frequency $\Delta\omega_i^n = \mathrm{Re}[\omega_i^n] - 1/\tau$ depending on the magnitude of the external field H_0 for $\alpha = 0.01$, $\tau\omega_K = 0.01$, $\omega_\Lambda/\omega_K = 10$: (*a*) the field is directed along the easy axis; (*b*) the field is directed perpendicular to the easy axis.

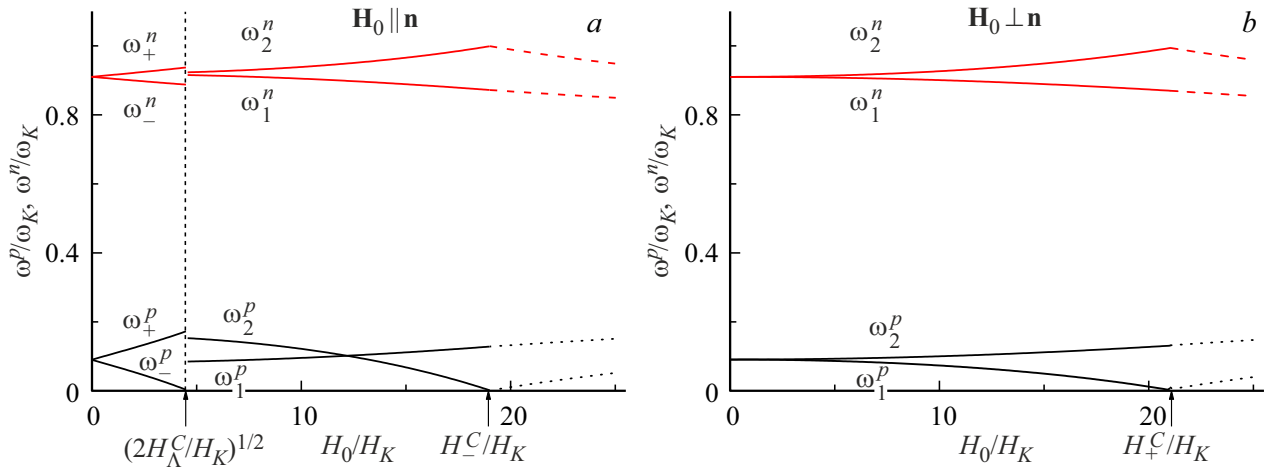

Figure 3. Imaginary parts $\omega_i''^{p,n} = \mathrm{Im}[\omega_i^{p,n}]$ of the complex frequencies of precession and nutation of the AFM magnetization depending on the magnitude of the external field H_0 for $\alpha = 0.01$, $\tau\omega_K = 0.01$, $\omega_\Lambda/\omega_K = 10$: (*a*) the field is directed along the easy axis; (*b*) the field is directed perpendicular to the easy axis.

are related as $\lambda_k = -i\omega_k$. The solution of the matrix Eq. (22) can be formally written as

$$\mathbf{X} = (\omega^2\mathbf{I} - i\omega\mathbf{D} - \mathbf{V})^{-1}\mathbf{F}. \tag{24}$$

The solution of Eq. (24) allows the determination of the components of the complex susceptibility tensor $\chi_{GG} = \chi'_{GG} - i\chi''_{GG}$ $(G = X, Y, Z)$.

Let's direct the alternating field along one of the axes X, Y, Z and consider the projection of the magnetization on this axis. The following expressions are valid for the projections of the magnetization

$$M_X(t)/M_0 = \sum_{i=1,2} \sin\vartheta_i(t)\cos\varphi_i(t)$$

$$= M_X^C(t)/M_0 + \chi_{XX}(\omega)\exp[i\omega t], \tag{25}$$

$$M_Y(t)/M_0 = \sum_{i=1,2} \sin\vartheta_i(t)\sin\varphi_i(t)$$

$$= M_Y^C(t)/M_0 + \chi_{YY}(\omega)\exp[i\omega t], \tag{26}$$

$$M_Z(t)/M_0 = \sum_{i=1,2} \cos\vartheta_i(t) = M_Z^C(t)/M_0 + \chi_{ZZ}(\omega)\exp[i\omega t]. \tag{27}$$

The constant components in the expressions (25)–(27) are defined as (they can be zero in various configurations)

$$M_X^C/M_0 = \sum_{i=1,2} \sin\vartheta_i^{\min}\cos\varphi_i^{\min}, \tag{28}$$

$$M_Y^C/M_0 = \sum_{i=1,2} \sin\vartheta_i^{\min}\sin\varphi_i^{\min}, \tag{29}$$

$$M_Z^C/M_0 = \sum_{i=1,2} \cos\vartheta_i^{\min}. \tag{30}$$

The components of the susceptibility tensor $\chi_{GG}(\omega)$ are expressed in terms of the elements of the vector $\mathbf{X}$, namely through $\Delta\vartheta_i$ and $\Delta\varphi_i$, as

$$\chi_{XX}(\omega) = \sum_{i=1,2} (\cos\vartheta_i^{\min}\cos\varphi_i^{\min}\Delta\vartheta_i - \sin\vartheta_i^{\min}\sin\varphi_i^{\min}\Delta\varphi_i), \tag{31}$$

$$\chi_{YY}(\omega) = \sum_{i=1,2} (\cos\vartheta_i^{\min}\sin\varphi_i^{\min}\Delta\vartheta_i + \sin\vartheta_i^{\min}\cos\varphi_i^{\min}\Delta\varphi_i), \tag{32}$$

$$\chi_{ZZ}(\omega) = -\sum_{i=1,2} \sin\vartheta_i^{\min}\Delta\vartheta_i, \tag{33}$$

5. Results and discussion

Figure 2 shows the precession frequencies $\omega'^p_i = \mathrm{Re}[\omega^p_i]$ of the total magnetization of the AFM sublattices and the deviations $\Delta\omega^n_i = \mathrm{Re}[\omega^n_i] - \tau^{-1}$ of the nutation frequencies of the magnetization of the AFM sublattices from the fundamental frequency set by the inverse value of the inertial relaxation time τ^{-1}, depending on the magnitude of the external field H_0. The values of $\Delta\omega^n_i$ depend on the field H_Λ attributable to the exchange interaction and on the field H_K attributable to the magnetic anisotropy. The sharp changes of the curves shown in Figure 2 at $H_0 = \sqrt{2H_\Lambda H_K}$ and at $H_0 = H^C_\pm = 2H_\Lambda \pm H_K$ are explained by transitions between AFM states („spin-flop“ and „spin-flip“ transitions) and are analogous to similar changes observed for precessional frequencies [2]. It should be noted that in inertial corrections in the expressions for some eigenfrequencies of AFM a factor with a dimensionless multiplier $\tau\omega^C_\pm \sim 2\tau\omega_\Lambda$ dominates (see Table 3), whereas a similar multiplier in FM is formally estimated as $\tau\omega^C_\pm = \tau\omega_K$ ($\omega_\Lambda = 0$). Since $\omega_\Lambda \gg \omega_K$ is common in AFMs, such inertial corrections in an AFM are significantly larger than the corresponding corrections for the eigenfrequencies of a FM. This effect of increasing the contribution of inertia to the correction for the eigenfrequencies of an AFM compared to a FM was noted in Ref.[26] when considering the case (a). However, as follows from Table 3, it is not observed in other states for all eigenfrequencies (see, for example, the expression for $\omega^{p,n}_1$ in the case (c)).

Figure 3 shows the imaginary parts of the complex frequencies of precession and nutation of the AFM magnetization as a function of the magnitude of the external field H_0. It should be noted that the imaginary parts of the complex expressions for the eigenfrequencies of the AFM determine the half-widths of the resonant lines observed at these frequencies. As can be seen from Figure 3, an increase of the magnitude of the external field leads to a change (increase or decrease, depending on the selected mode) of the half-width of the NR lines. Moreover, a half-width change is observed in case of the „spin-flop“ transition.

Figure 4 shows the frequency dependences of the real χ'_{ZZ} and imaginary χ''_{ZZ} parts of the AFM linear susceptibility tensor χ_{ZZ} in the case (a). A general precession

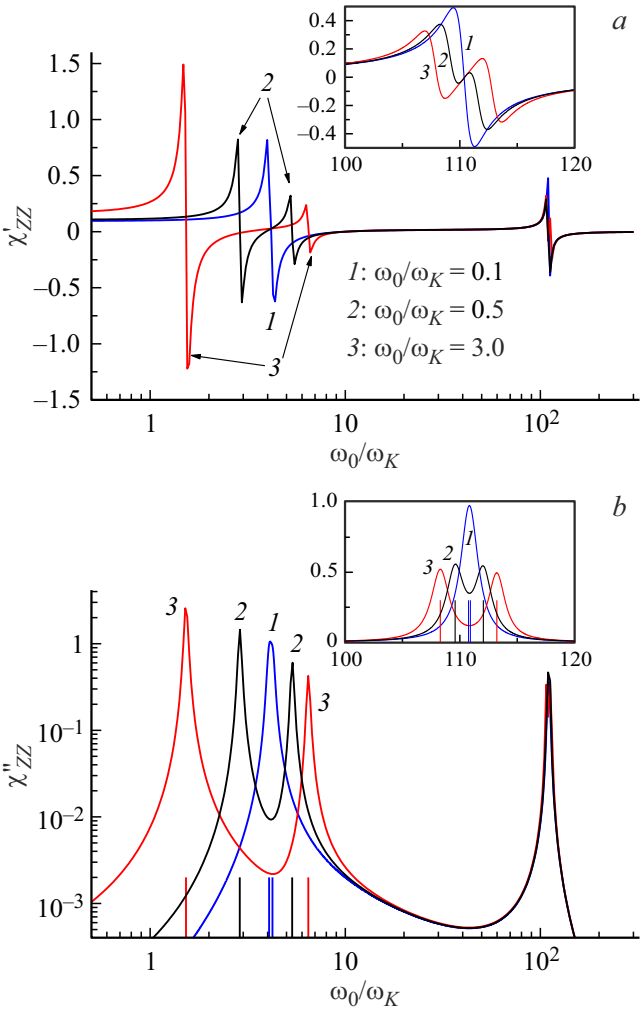

Figure 4. Realχ'_{ZZ} (a) and imaginary χ''_{ZZ} (b) parts of the linear susceptibility tensor component $\chi_{ZZ} = \chi'_{ZZ} - i\chi''_{ZZ}$ (Eq. (33)) AFM depending on ω/ω_K for $\alpha = 0.01$, $\tau\omega_K = 0.001$, $\omega_\Lambda/\omega_K = 10$ and various values of ω_0/ω_K corresponding to the state (a). Frequency labels are solutions of equation (a) from Table 2 for $\alpha = 0$.

of the sublattice magnetization is observed in a weak external field, which leads to the occurrence of only one AFM peak. The AFMR is divided into two peaks with an increase of the external field relative to the anisotropy field. The frequencies of these resonances can be estimated as $\omega^p_\pm \sim \sqrt{\omega_K\omega^C_+} \pm \omega_0$ (for a more accurate estimate (see Table 3, case (a)). As can be seen in Figure 4, a weaker paired NR appears at frequencies exceeding by two orders of magnitude the frequency of the AFM resonance $\omega^n_\pm \sim \tau^{-1} + \omega_K + \omega_\Lambda \pm \omega_0$ in addition to the paired antiferromagnetic resonance caused by the precessional motion of the magnetization of the AFM sublattices. The frequency separation between the peaks decreases as the magnitude of the external field H_0 decreases, and they merge at $\omega_0 = \gamma H_0 = 0$. It can be seen from the expressions for the resonance frequencies that the relative frequency shift of NR due to the external field $\Delta\omega^n_\pm/\tau^{-1} \sim \tau\omega_0$ is not

as significant as the similar relative frequency shift of AFM resonance $\Delta\omega_{\pm}^{p}/\sqrt{\omega_K\omega_{+}^{C}} \sim \omega_0/\sqrt{\omega_K\omega_{+}^{C}}$. The inertial correction to AFM resonance frequencies is estimated as $\sim \tau\omega_\Lambda(\omega_K\omega_\Lambda)^{1/2}$ according to the expression for $\omega_{\pm}^{p}$ from Table 3 (case (a)). This correction can be compared with the inertial correction to FM resonance frequencies, which can be formally estimated as $\sim \tau\omega_K^2$ if we put $\omega_\Lambda = 0$ in the expressions for $\omega_{\pm}^{p}$. Thus, the ratio of correction values is determined by the frequency ratio as $\sim (\omega_\Lambda/\omega_K)^{3/2}$, which means that the inertial correction for AFM is significantly greater than for FM, since $\omega_\Lambda \gg \omega_K$ [24].

Figure 5 and 6 show the dependencies for the components of the susceptibility tensor for the states (b) and (d), respectively. Figure 5 shows that as the magnitude of the external field increases, the resonant frequencies $\omega_1^{p,n}$ (see Table 3, case (b)) shift to the high-frequency region for $\chi_{ZZ}(\omega)$, whereas the resonant frequencies ω_2^{n} are shifted to the low frequency range for $\chi_{YY}(\omega)$. A similar picture is observed in Figure 6, where, with an increase of the magnitude of the external field, the resonant frequencies $\omega_1^{p,n}$ (see Table 3, case (d)) are shifted to the high frequency range for $\chi_{ZZ}(\omega)$, and the resonant frequencies $\omega_2^{p,n}$ are shifted to the low frequency range for $\chi_{XX}(\omega)$.

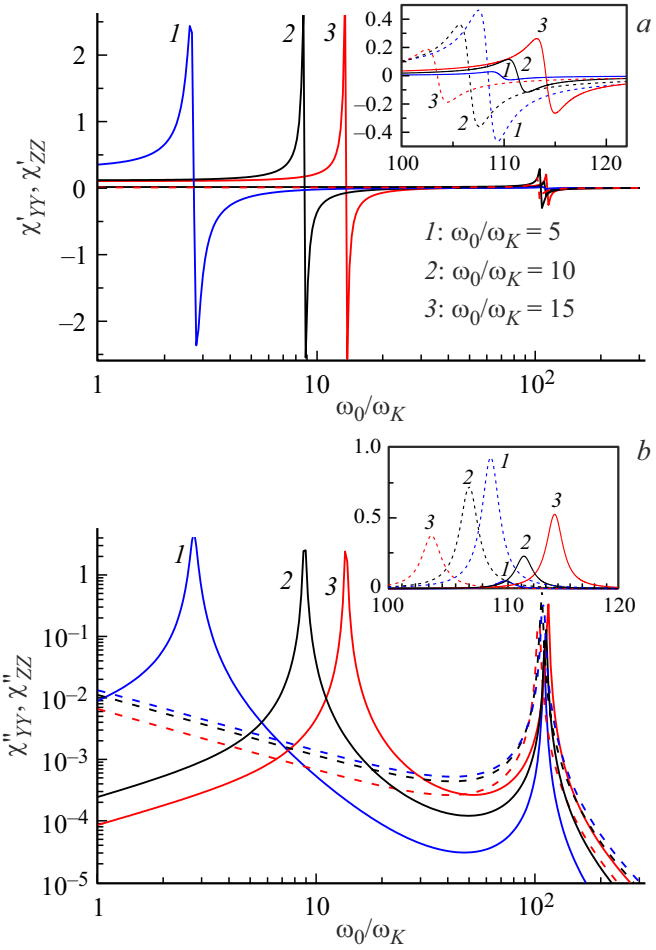

Figure 5. Realχ'_{GG} (a) and imaginary χ''_{GG} (b) parts of the linear susceptibility tensor component $\chi_{GG} = \chi'_{GG} - i\chi''_{GG}$ (Eq. (33)) of AFM depending on ω/ω_K for $\alpha = 0.01$, $\tau\omega_K = 0.001$, $\omega_\Lambda/\omega_K = 10$ and various values of ω_0/ω_K corresponding to the state (b). Solid lines: $G = Z$, dashed lines: $G = Y$.

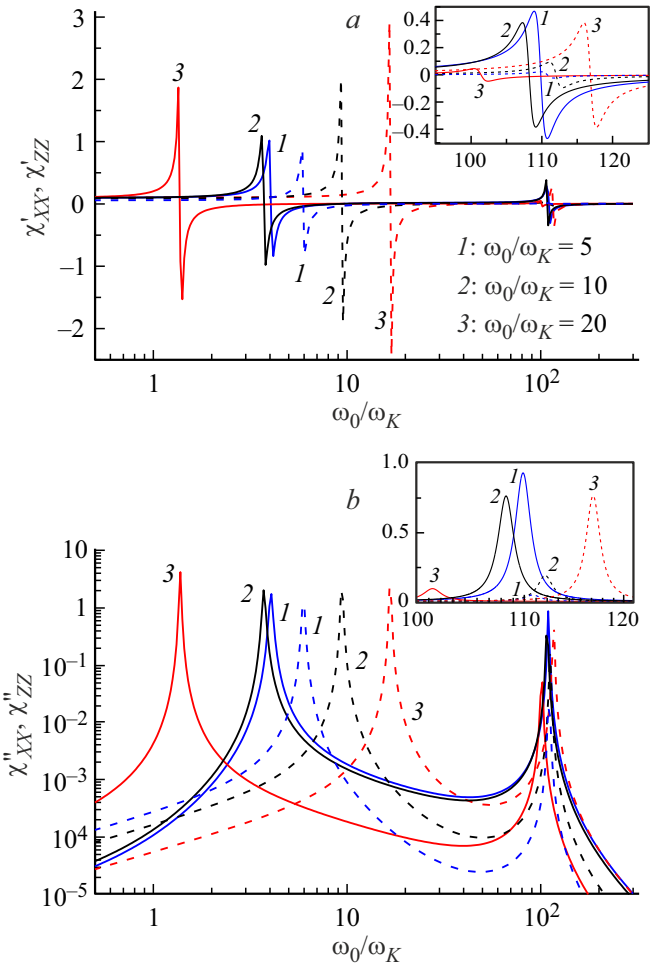

Figure 6. Realχ'_{GG} (a) and imaginary χ''_{GG} (b) parts of the linear susceptibility tensor component $\chi_{GG} = \chi'_{GG} - i\chi''_{GG}$ (Eq. (33)) of AFM depending on ω/ω_K for $\alpha = 0.01$, $\tau\omega_K = 0.001$, $\omega_\Lambda/\omega_K = 10$ and various values of ω_0/ω_K corresponding to the state (d). Solid lines: $G = X$, dashed lines: $G = Z$.

6. Conclusion

The method of linearization of the system of inertial LLG equations describing the inertial dynamics of the magnetization of AFM sublattices, taking into account the dissipation in them, enables one to obtain analytical expressions for the eigenfrequencies of AFM. The real parts of these expressions determine the frequencies of both antiferromagnetic resonance and NR, while the imaginary parts affect the half-widths of these resonance lines. The dependences of both the resonant frequencies and the half-widths of the lines on the magnitude of the external field are presented, taking into account the dissipation in

the AFM material. It is shown that the direction of the shift of the resonant frequencies with the increase of the field depends on the AFM state and the considered resonant mode in this state. The individual components of the AFM magnetization tensor in the inertial regime are calculated. It is demonstrated how switching the AFM state by an external field impacts the NR frequencies in the AFM. The expressions obtained also make it possible to evaluate the effect of magnetization inertia on resonant frequencies and half-widths of lines in various AFM states. It is noted that the more inertial corrections there are for FM, the greater the ratio ω_Λ/ω_K in different AFM states for individual resonant modes. A decrease of the half-width of NR lines on individual modes by an external field (see Figure 3) while maintaining the area under the resonance curve (Gordon's integral rule [45]) leads to an increase of the resonance amplitude, which may be useful in developing a technique for experimental observation of nutation resonances. Moreover, the effective half-width of the nutation resonance line, defined as the ratio of the imaginary part of the complex resonant frequency (see Table 3) to its real part $\mathrm{Im}[\omega_i^n]/\mathrm{Re}[\omega_i^n]$, decreases in some AFM states with the increase of the ratio $H_\Lambda/H_K = \Lambda/2K$. Accordingly, the resonance amplitude will be greater in such an AFM, which makes them more convenient for observing the nutation resonance [26]. For example, such an AFM include structures containing NiO [46,47] and CrPt [48,49]. The results obtained correspond to weak external variable fields (the condition for linearization of the equations). The fact that AFM and ferrimagnets have a similar magnetic ordering nature [6,26] allows the generalization of the presented method for analyzing the resonant frequencies of ferrimagnets. In the future, it is of interest to study nonlinear corrections to the components of the linear susceptibility tensor and to study nonlinear effects in AFM in the field of nutation resonance. The results of the study of nonlinear effects in FM under the conditions of inertial dynamics of magnetization can be used as a basis [50]. We hope that the presented results will be useful in setting up future experiments for the study of NR in AFM structures.

Funding

The work was supported by the Foundation for the Advancement of Theoretical Physics and Mathematics „BASIS“ (grant: 22-1-1-28-1). Part of the work (A.F.) was carried out within the framework of the state assignment of the Kotelnikov Institute of Radio Engineering and Electronics of the Russian Academy of Sciences.

Conflict of interest

The authors declare that they have no conflict of interest.

References

[1] T. Jungwirth, X. Marti, P. Wadley, J. Wunderlich. Nat. Nanotechnol. **11**, 231 (2016). https://doi.org/10.1038/nnano.2016.18
[2] V. Baltz, A. Manchon, M. Tsoi, T. Moriyama, T. Ono, Y. Tserkovnyak. Rev. Mod. Phys. **90**, 015005 (2018). https://doi.org/10.1103/RevModPhys.90.015005
[3] M. Jungfleisch, W. Zhang, A. Hoffmann. Phys. Lett. A **382**, 865 (2018). https://doi.org/10.1016/j.physleta.2018.01.008
[4] Y.L. Raikher, V.I. Stepanov. ZhETF, **134**, 514 (2008). (in Russian). https://doi.org/10.1134/S1063776108090112
[5] P. Němec, M. Fiebig, T. Kampfrath, A.V. Kimel. Nat. Phys. **14**, 229 (2018). https://doi.org/10.1038/s41567-018-0051-x
[6] A.G. Gurevich. Magnitnyi rezonans v ferritakh i antiferomagnetikakh. (Nauka, M. (1973). (in Russian).
[7] L.D. Landau. Phys. Zs. Sowjet **4**, 675 (1933). https://elib.biblioatom.ru/text/landau_sobranie-trudov_t1_1969/p100/
[8] L. Néel. C.R. Hebd. Seances Acad. Sci. **252**, 4075 (1961). https://hal.science/hal-02878431/document.
[9] L. Néel. C.R. Hebd. Seances Acad. Sci. **253**, 9 (1961). https://hal.science/hal-02878448v1/file/Doc.pdf
[10] L. Néel. C.R. Hebd. Seances Acad. Sci. **253**, 203 (1961). https://hal.science/hal-02878449/document
[11] L. Néel. C.R. Hebd. Seances Acad. Sci. **253**, 1286 (1961). https://hal.science/hal-02878450
[12] Handbook of Terahertz Technology for Imaging, Sensing and Communications / Ed. D. Saeedkia. Woodhead Publ. Lim., Sawston (2013).
[13] J.-Y. Bigot, M. Vomir, E. Beaurepaire. Nat. Phys. **5**, 515 (2009). https://doi.org/10.1038/nphys1285
[14] C.D. Stanciu, A. Tsukamoto, A.V. Kimel, F. Hansteen, A. Kirilyuk, A. Itoh, Th. Rasing. Phys. Rev. Lett. **99**, 217204 (2007). https://doi.org/10.1103/PhysRevLett.99.217204
[15] S. Mangin, M. Gottwald, C-H. Lambert, D. Steil, V. Uhlíř, L. Pang, M. Hehn, S. Alebrand, M. Cinchetti, G. Malinowski, Y. Fainman, M. Aeschlimann, E.E. Fullerton. Nature Mater **13**, 286 (2014). https://doi.org/10.1038/nmat3864
[16] A. Kimel, B. Ivanov, R. Pisarev, P.A. Usachev, A. Kirilyuk, Th. Rasing. Nature Phys. **5**, 727 (2009). https://doi.org/10.1038/nphys1369
[17] S. Wienholdt, D. Hinzke, U. Nowak. Phys. Rev. Lett. **108**, 247207 (2012). https://doi.org/10.1103/PhysRevLett.108.247207
[18] M.-C. Ciornei, J.M. Rubí, J.-E. Wegrowe. Phys. Rev. B **83**, 020410(R) (2011). https://doi.org/10.1103/PhysRevB.83.020410
[19] J.-E. Wegrowe, M.-C. Ciornei. Amer. J. Phys. **80**, 607 (2012). https://doi.org/10.1119/1.4709188
[20] D. Böttcher, J. Henk. Phys. Rev. B **86**, 020404(R) (2012). https://doi.org/10.1103/PhysRevB.86.020404
[21] S. Giordano, P.-M. Déjardin. Phys. Rev. B **102**, 214406 (2020). https://doi.org/10.1103/PhysRevB.102.214406
[22] E. Olive, Y. Lansac, J.-E. Wegrowe. Appl. Phys. Lett. **100**, 192407 (2012). https://doi.org/10.1063/1.4712056
[23] S.V. Titov, W.J. Dowling, Yu.P. Kalmykov. J. Appl. Phys. **131**, 193901 (2022). https://doi.org/10.1063/5.0093226
[24] M. Cherkasskii, M. Farle, A. Semisalova. Phys. Rev. B **102**, 184432 (2020). https://doi.org/10.1103/PhysRevB.102.184432

[25] S. Ghosh, M. Cherkasskii, I. Barsukov, R. Mondal, Theory of tensorial magnetic inertia in terahertz spin dynamics (2024). https://doi.org/10.48550/arXiv.2408.15594
[26] R. Mondal, S. Großenbach, L. Rózsa, U. Nowak. Phys. Rev. B **103**, 104404 (2021). https://doi.org/10.1103/PhysRevB.103.104404
[27] S.V. Titov, W.J. Dowling, A.S. Titov, A.S. Fedorov. J. Appl. Phys. **135**, 093903 (2024). https://doi.org/10.1063/5.0196622
[28] M. Cherkasskii, M. Farle, A. Semisalova. Phys. Rev. B, **103**, 174435 (2021). https://doi.org/10.1103/PhysRevB.103.174435
[29] A.M. Lomonosov, V.V. Temnov, J.-E. Wegrowe. Phys. Rev. B, **104**, 054425 (2021). https://doi.org/10.1103/PhysRevB.104.054425
[30] S.V. Titov, W.J. Dowling, Y.P. Kalmykov, M. Cherkasskii. Phys. Rev. B, **105**, 214414 (2022). https://doi.org/10.1103/PhysRevB.105.214414
[31] R. Mondal, L. Rózsa. Phys. Rev. B **106**, 134422 (2022). https://doi.org/10.1103/PhysRevB.106.134422
[32] K. Neeraj, N. Awari, S. Kovalev, D. Polley, N.Z. Hagström, S.S.P.K. Arekapudi, A. Semisalova, K. Lenz, B. Green, J.-C. Deinert, I. Ilyakov, M. Chen, M. Bowatna, V. Scalera, M. D'Aquino, C. Serpico, O. Hellwig, J.-E. Wegrowe, M. Gensch, S. Bonetti. Nat. Phys. **17**, 245 (2021). https://doi.org/10.1038/s41567-020-01040-y
[33] A. De, J. Schlegel, A. Lentfert, L. Scheuer, B. Stadtmüller, P. Pirro, G. von Freymann, U. Nowak, M. Aeschlimann. Nutation: separating the spin from its magnetic moment (2024). https://doi.org/10.48550/arXiv.2405.01334
[34] V. Unikandanunni, R. Medapalli, M. Asa, E. Albisetti, D. Petti, R. Bertacco, E.E. Fullerton, S. Bonetti. Phys. Rev. Lett. **129**, 237201 (2022). https://doi.org/10.1103/PhysRevLett.129.237201
[35] D. Thonig, O. Eriksson, and M. Pereiro, Sci. Rep. **7**, 931 (2017). https://doi.org/10.1038/s41598-017-01081-z
[36] M. Fähnle, D. Steiauf, C. Illg. Phys. Rev. B **84**, 172403 (2011). https://doi.org/10.1103/PhysRevB.84.172403
[37] S. Bhattacharjee, L. Nordström, J. Fransson. Phys. Rev. Lett. **108**, 057204 (2012). https://doi.org/10.1103/PhysRevLett.108.057204
[38] R. Mondal, M. Berritta, A.K. Nandy, P.M. Oppeneer. Phys. Rev. B **96**, 024425 (2017). https://doi.org/10.1103/PhysRevB.96.024425
[39] T. Kikuchi, G. Phys. Rev. B **92**, 184410 (2015). https://doi.org/10.1103/PhysRevB.92.184410
[40] R. Bastardis, F. Vernay, H. Kachkachi, Phys. Rev. B **98**, 165444 (2018). https://doi.org/10.1103/PhysRevB.98.165444
[41] M. Cherkasskii, I. Barsukov, R. Mondal, M. Farle, A. Semisalova. Phys. Rev. B **106**, 054428 (2022). https://doi.org/10.1103/PhysRevB.106.054428
[42] W.T. Coffey, Yu.P. Kalmykov, S.V. Titov. Thermal Fluctuations and Relaxation Processes in Nanomagnets, World Scientific, Singapore (2020).
[43] R. Bellman. Introduction to matrix analysis, McGraw-Hill, N.Y. (1960).
[44] G.A. Korn, T.M. Korn. Mathematical Handbook for Scientists and Engineers: Definitions, Theorems, and Formulas for Reference and Review, McGraw-Hill, N.Y. (1961).
[45] S.V. Titov, W.J. Dowling, A.S. Titov, S.A. Nikitov, M.A. Cherkasskii. Phys. Rev. B, **107**, 104416 (2023). https://doi.org/10.1103/PhysRevB.107.104416
[46] M.T. Hutchings, E.J. Samuelsen. Phys. Rev. B **6**, 3447 (1972). https://doi.org/10.1103/PhysRevB.6.3447
[47] T. Satoh, S.-J. Cho, R. Iida, T. Shimura, K. Kuroda, H. Ueda, Y. Ueda, B.A. Ivanov, F. Nori, and M. Fiebig, Phys. Rev. Lett. **105**, 077402 (2010). https://doi.org/10.1103/PhysRevLett.105.077402
[48] M.J. Besnus, A.J.P. Meyer. Physica Status Solidi B **58**, 533 (1973). https://doi.org/10.1002/pssb.2220580213
[49] R. Zhang, R. Skomski, X. Li, Z. Li, P. Manchanda, A. Kashyap, R.D. Kirby, S.-H. Liou, D.J. Sellmyer. J. Appl. Phys. **111**, 07D720 (2012). https://doi.org/10.1063/1.3677928
[50] S.V. Titov, W.J. Dowling, A.S. Titov, A.S. Fedorov. AIP Advances, **14**, 035216 (2024). https://doi.org/10.1063/5.0191413

Translated by A.Akhtyamov